Eur. Phys. J. C (2019) 79:518
https://doi.org/10.1140/epjc/s10052-019-7005-z

THE EUROPEAN PHYSICAL JOURNAL C

Regular Article - Theoretical Physics

NLO Productions of ω and K^0_S with a global extraction of the jet transport parameter in heavy-ion collisions

Guo-Yang Ma[1], **Wei Dai**[2,a], **Ben-Wei Zhang**[1,b], **Enke Wang**[1]

[1] Key Laboratory of Quark and Lepton Physics (MOE) and Institute of Particle Physics, Central China Normal University, Wuhan 430079, China
[2] School of Mathematics and Physics, China University of Geosciences, Wuhan 430079, China

Received: 6 December 2018 / Accepted: 1 June 2019 / Published online: 17 June 2019

Abstract In this work, we pave the way to calculate the productions of ω and K^0_S mesons with large p_T in p+p and A+A collisions both at RHIC and LHC. The fragmentation functions (FFs) of the ω meson in vacuum at next-to-leading order (NLO) are obtained by evolving the NLO DGLAP evolution equations with rescaled ω FFs at initial scale $Q_0^2 = 1.5\ \mathrm{GeV}^2$ from a broken SU(3) model, and the FFs of K^0_S in vacuum are taken from AKK08 parametrization directly. Within the framework of the NLO pQCD improved parton model, we arrive at good descriptions of the experimental data on ω and K^0_S in p+p both at RHIC and LHC. With the higher-twist approach, to take into account jet quenching effect by medium-modified FFs, nuclear modification factors for ω meson and K^0_S meson both at RHIC and LHC are presented with different sets of jet transport coefficients $\hat{q}_0$. Then we make a global extraction of $\hat{q}_0$ both at RHIC and LHC by confronting our model calculations with all available data on six identified mesons: π^0, η, ρ^0, ϕ, ω, and K^0_S. The minimum value of total $\chi^2/d.o.f$ for productions of these mesons gives the best value of $\hat{q}_0 = 0.5\ \mathrm{GeV}^2/\mathrm{fm}$ for Au+Au collisions with $\sqrt{s_{\mathrm{NN}}} = 200\,\mathrm{GeV}$ at RHIC, and $\hat{q}_0 = 1.2\,\mathrm{GeV}^2/\mathrm{fm}$ for Pb+Pb collisions with $\sqrt{s_{\mathrm{NN}}} = 2.76\,\mathrm{TeV}$ at LHC, respectively, with the QGP spacetime evolution given by the event-by-event viscous hydrodynamics model IEBE-VISHNU. With these global extracted values of $\hat{q}_0$, nuclear modification factors of π^0, η, ρ^0, ϕ, ω, and K^0_S in A+A collisions are presented, and predictions of yield ratios such as ω/π^0 and K^0_S/π^0 at the high-p_T regime in heavy-ion collisions both at RHIC and LHC are provided.

1 Introduction

The jet quenching effect describes energy dissipation of an energetic parton when it traverses through the hot and dense QCD medium, which is produced shortly after high energy nuclear collisions [1]. The single hadron production suppression at the high-p_T regime when compared to scaled p+p data is one of the primary perturbative probes to study the properties of this de-coupled quark and gluon QCD matter [2]. π^0 is the best measured final-state hadron, and its nuclear modification factor R_{AA} as a function of transverse momentum p_T is interpreted as the consequence of the jet quenching effect and it did help us to constrain the strength of the jet–medium interaction and the properties of the QCD medium [3–9]. In 2013, the Jet Collaboration summarized different jet quenching theoretical frameworks and compared the jet transport parameter extracted by different energy loss models using the same hydro description of QCD medium [10]. Meanwhile, the R_{AA} for different final-state identified hadrons have been measured, and their production suppressions as well as patterns of their yield ratios have been observed [4,5,11–16]. It is of interest and it is a challenge to describe the cross sections of leading hadrons of different types and their yield ratios with each other in heavy-ion collisions (HIC) both at RHIC and LHC with a unified model of jet quenching, which should shed light on the flavor dependence of the parton energy loss and the intrinsic properties of the identified hadron productions in p+p and A+A reactions [17–24].

We have achieved a better understanding of the suppression patterns of different mesons by conducting calculations and by analysis of the R_{AA} and particle ratios for other identified hadron productions [25–27]. We find that understanding of the suppression pattern of the leading hadron requires one to take into account all three factors [25]: the initial hard jet spectrum, the energy loss mechanism and the parton fragmentation functions in vacuum. The flavor dependence of the energy loss will result in a decrease of the fraction of

[a] e-mail: weidai@cug.edu.cn
[b] e-mail: bwzhang@mail.ccnu.edu.cn

gluon fragmenting contribution in the nuclear–nuclear collision and an increase of the fraction of the quark fragmenting contribution. The productions of final-state mesons, like π^0, ρ^0, η [25–27], are dominated by the quark fragmentation contribution at the high-p_T regime in p+p collisions. The energy loss effect will only enhance the domination of the quark fragmenting contribution in A+A collisions. Therefore ρ^0/π^0 and η/π^0 in p+p and A+A collisions coincide at large-p_T, since they are only determined by the ratios of the FFs in vacuum. But the production of ϕ meson is dominated by the gluon fragmenting contribution in p+p collision, therefore we can observe a separation of ϕ/π^0 in p+p and A+A. It is of great interest to gain better understanding of the suppression pattern of different final-state hadrons, and furthermore to provide systematical pQCD predictions for the current experimental measurement of the identified hadrons. In this letter, we mainly investigate one of the low-mass vector mesons (ω) and one of the pseudoscalar mesons (K^0_S), together with π^0, η, ρ^0 and ϕ to achieve these goals.

In this article, we investigate the production of two other mesons, ω and K^0_S, with large p_T in A+A collisions, which has never been computed so far, to the best of our knowledge. The ω meson is constituted of a similar valence quark of π^0 with larger mass 782.65 MeV and spin 1. Kaons are a group of lightest mesons, carrying strangeness components, $K^0_S(\frac{d\bar{s}+s\bar{d}}{2})$ is one type of kaon, consisting of s-quark, d-quark and their corresponding anti-quarks. The productions of these two mesons have been measured in p+p and A+A collisions both at RHIC and LHC, but a theoretical description is lacking. Within the NLO pQCD improved parton model, we calculate ω and K^0_S yields at the high-p_T regime in heavy-ion collisions, by employing medium-modification fragmentation functions (FFs) due to gluon radiation in the hot/dense QCD medium in the higher-twist approach of jet quenching [22,23,28–30], the same approach as in our calculations on the productions of η, ρ^0 and ϕ mesons in HIC [25–27].

It is noted in the previous studies that, for consistency, we implemented the Hirano hydro description [31,32] to describe the spacetime evolution of the QGP fireball. In this work, we utilize a state-of-the-art, event-by-event (2+1)-D viscous hydrodynamics model (IEBE-VISHNU) [33] to give the spacetime evolution information of the hot and dense medium. Due to the changes of the medium description, the strength of the jet–medium interaction characterized by the jet transport parameter $\hat{q}_0$ should be re-extracted. Taking advantage of the systematical study of the nuclear modification factors with respect to p_T and the large amount of experimental data of π^0, η, ρ^0 and ϕ both at RHIC and LHC, with two more mesons ω and K^0_S calculated in this article, we can make a global extraction of the jet transport parameter $\hat{q}_0$ with all the available experimental data of these six identified mesons $R_{\rm AA}$.

The article is organized as follows. We first present the theoretical framework of computing single hadron cross sections in p+p collision in Sect. 2, and we give the p+p baseline in investigating the in-medium modification of these productions. In Sect. 3, we discuss the inclusive hadron production in A+A collisions with the medium-modified FFs, based on the higher-twist approach of parton energy loss, and we present the nuclear modification factors $R_{\rm AA}$ for ω and K^0_S both at RHIC and LHC. Section 4 shows the global extraction of the jet transport coefficient $\hat{q}_0$ both at RHIC and LHC by confronting our model calculations with all available data on six identified mesons: π^0, η, ρ^0, ϕ, ω, and K^0_S. In Sect. 5, we make predictions on the identified hadron yield ratios ω/π^0 and K^0_S/π^0 in p+p and A+A collisions, and we compare them with experimental data if applicable. We give a brief summary in Sect. 6.

2 Large $p_{\rm T}$ yield of ω and K^0_S meson in p+p

We start with the productions of ω and K^0_S mesons at NLO in p+p collisions. In the framework of the pQCD improved parton model, the inclusive hadron production in p+p collisions can be given by the convolution of three parts, the parton distribution functions (PDFs) in a proton, the hard partonic scattering cross section, denoted $d\sigma/d\hat{t}$ (up to the order of α_s^3), and the parton fragmentation functions (FFs) to the final-state hadron $D_{q(g)\to h}(z_h, Q^2)$. One may convolute PDFs and partonic cross section $d\sigma/d\hat{t}$ into the initial hard (parton-) jet spectrum $F_{q,g}(p_T)$, and we have

$$\frac{1}{p_T}\frac{{\rm d}\sigma_{\omega,K^0_S}}{{\rm d}p_T} = \int F_q\left(\frac{p_T}{z_h}\right)\cdot D_{q\to\omega,K^0_S}(z_h, p_T)\frac{{\rm d}z_h}{z_h^2} + \int F_g\left(\frac{p_T}{z_h}\right)\cdot D_{g\to\omega,K^0_S}(z_h, p_T)\frac{{\rm d}z_h}{z_h^2}. \quad (1)$$

Here, the quark and gluon fragmenting contributions are written separately to facilitate future discussions. A next-to-leading order (NLO) Monte Carlo code has been employed to calculate leading hadron productions in the p+p collision [36], and the CT14 parametrization of PDFs for the free proton [37] has been implemented. In the framework, as long as the parametrization of the specific final-state hadron FFs in vacuum is available, one can predict its production yield at large $p_{\rm T}$ in elementary p+p collisions in principle.

In order to make the NLO calculation of ω and K^0_S mesons in p+p, the NLO parton FFs of these two mesons are needed. The parton FFs of the K^0_S meson at NLO can be found in the AKK08 parametrization [38], while there is not such a kind of global parametrization for ω FFs in vacuum. So we have to rely on theoretical models and utilize ω parton FFs at a starting scale $Q_0^2 = 1.5\,{\rm GeV}^2$ provided by a broken SU(3) model [39,40]. We note that our preceding investigations on leading

ρ^0 and ϕ production [26,27] have benefited from this broken SU(3) model. In this model, the independent parton FFs of different flavor are reduced into three independent functions named valence function, $V(x, Q_0^2)$, sea function, $\gamma(x, Q_0^2)$ and gluon function, $D_g(x, Q_0^2)$, by considering the SU(3) flavor symmetry with a symmetry breaking parameter and also addressing the isospin and charge conjugation invariance of the vector mesons. We can write these three functions into a standard polynomial at the starting low energy scale of $Q_0^2 = 1.5\ \mathrm{GeV}^2$ as

$$H_i(x) = a_i x^{b_i}(1-x)^{c_i}(1 + d_i x + e_i x^2), \tag{2}$$

where the full set of parameters (a, b, c, d, e) defined in V, γ, D_g and a few additional parameters defined for each vector meson such as the strangeness suppression factor λ, the vector mixing angle θ, the sea suppression factor $f_{\mathrm{sea}}^{\omega}$, $f_1^u(\omega)$ and f_g^{ω} have been determined in the broken SU(3) model in Refs. [39,40], and we multiply the parameter a_i by 3 to make the best fit to the yield of the ω meson in p+p collisions. All these parameters for fitting the initial FFs of ω meson are listed in Table 1. To obtain a NLO parton FF for ω at any energy scale Q, we employ the numerical NLO DGLAP evolution program provided in Ref. [41] with the initial parton FFs starting scale $Q_0^2 = 1.5\ \mathrm{GeV}^2$ as input.

We demonstrate in Fig. 1 the NLO DGLAP evolved FFs of the ω meson as functions of z_h at fixed $Q^2 = 1.5\ \mathrm{GeV}^2$ and $Q^2 = 100\ \mathrm{GeV}^2$ on the left and as functions of Q at fixed $z_h = 0.4$ and $z_h = 0.6$ on the right. We find in the typical fraction region ($z_h = 0.4 \to 0.7$) $D_g^{\omega} > D_s^{\omega} \gg D_{u(d)}^{\omega}$, unlike the case $D_s^{\phi} > D_g^{\phi} \gg D_{u(d)}^{\phi}$ in the ϕ FFs [27]. Due to the fact that in parton FFs the gluon contribution exceeds the quark contribution, an overwhelming advantage of the gluon fragmenting contribution of the final-state ω production in p+p collision is expected in the competition with the quark fragmenting contribution. In Fig. 2, we plot the NLO FFs of K_S^0 from the AKK08 parametrization in the same manner as the ω meson in Fig. 1. We find the strange quark FF $D_s^{K_S^0} > D_g^{K_S^0}$ in the typical $z_h = 0.4 \to 0.7$ region, therefore competition of the gluon and quark fragmenting contributions is expected in the K_S^0 production in p+p collisions based on the pattern discovered in the previous study of the π^0, η, ρ^0 and ϕ mesons.

With the NLO FFs in vacuum of both the ω and the K_S^0 mesons, we are able to confront the numerical results of the ω and K_S^0 meson productions in p+p collisions up to NLO with the available experimental data both at RHIC and LHC shown in Figs. 3 and 4. Note that, in our simulations, the hard scales such as factorization scale, renormalization scale and fragmentation scale are chosen to be the same and proportional to the p_T of the final-state hadron. We see that the numerical results match well with the experimental data on ω meson spectra both at RHIC, $\sqrt{s_{\mathrm{NN}}} = 200$ GeV, and LHC,

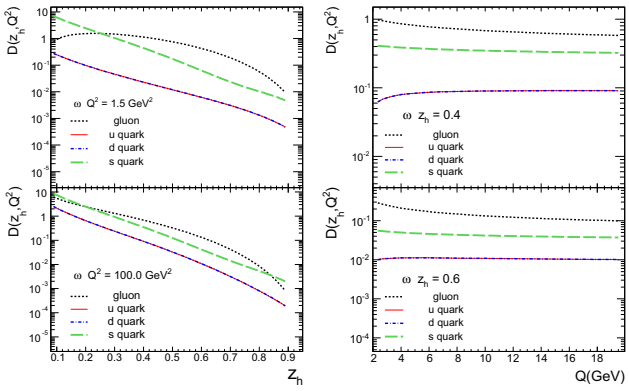

Fig. 1 Left: The NLO DGLAP evolved fragmentation functions of ω meson as functions of z_h at fixed $Q^2 = 1.5\ \mathrm{GeV}^2$ and $Q^2 = 100\ \mathrm{GeV}^2$. Right: The NLO DGLAP evolved fragmentation functions of ω meson as functions of Q at fixed $z_h = 0.4$ and $z_h = 0.6$

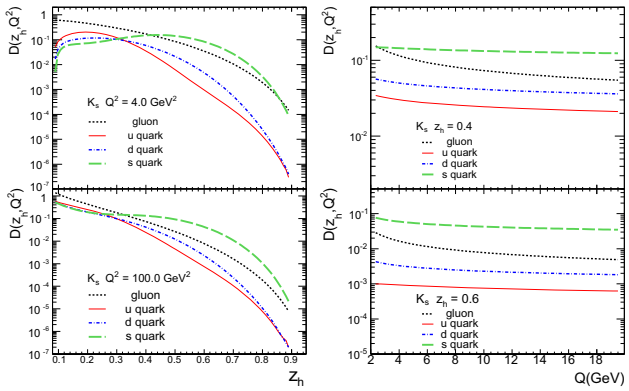

Fig. 2 Left: The NLO DGLAP evolved Fragmentation Functions of K_S^0 meson as functions of z_h at fixed $Q^2 = 4.0\ \mathrm{GeV}^2$ and $Q^2 = 100\ \mathrm{GeV}^2$. Right: The NLO DGLAP evolved fragmentation functions of K_s^0 meson as functions of Q at fixed $z_h = 0.4$ and $z_h = 0.6$

$\sqrt{s_{\mathrm{NN}}} = 7$ TeV, and the hard scales, $\mu = 0.5\ p_T$, as shown in Fig. 3. We also demonstrate in Fig. 4 the good agreement of the theoretical calculations of the leading K_S^0 meson with the STAR data and the ALICE data, where the hard scales are fixed to be $\mu = 1.0\ p_T$ to give the best fit.

3 Large p_T yield of ω and K_S^0 meson in A+A

To calculate the ω and K_S^0 productions in A+A collisions, the jet quenching effect should be included. In this article we utilize the higher-twist approach of parton energy loss, which relates the parton energy loss due to its multiple scattering in QCD medium and medium-induced gluon radiation to twist-four processes, and this shows that these processes give rise to additional terms in QCD evolution equations and lead to the effectively medium-modified fragmentation functions; thus the partonic energy loss effect can be taken into account by replacing the FFs in vacuum with the effec-

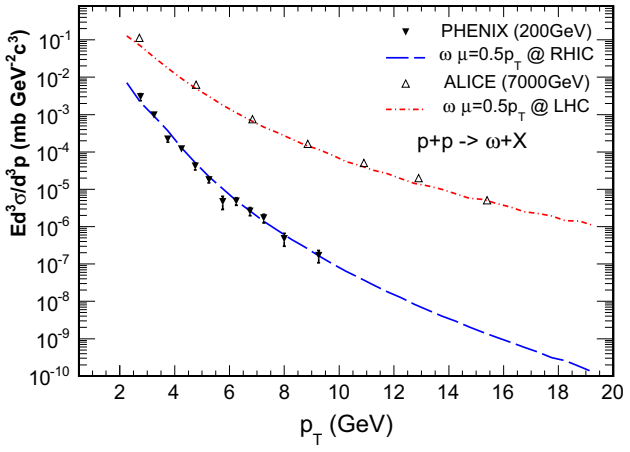

Fig. 3 The theoretical results of the ω meson production in p+p collisions at $\sqrt{s} = 200$ GeV confronted with the PHENIX data [15] and confronted with the ALICE data [34] at $\sqrt{s} = 7$ TeV

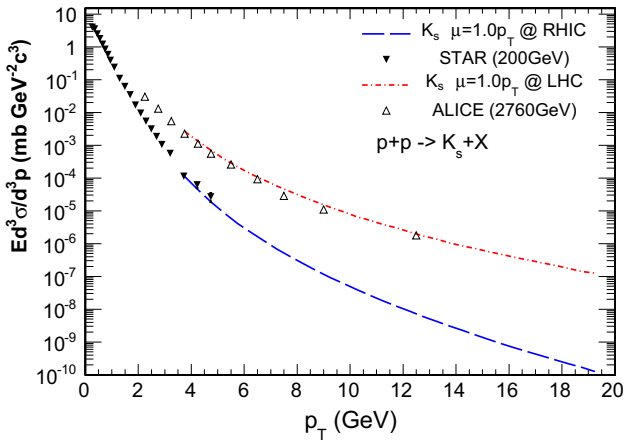

Fig. 4 The theoretical results of the K_s^0 meson production in p+p collisions at $\sqrt{s} = 200$ GeV RHIC compared with STAR data [35] and at $\sqrt{s} = 2.76$ TeV LHC compared with ALICE data [16]

tively medium-modified FFs [28–30,42,43]. By assuming a thermal ensemble of quasi-particle states in the hot/dense medium and neglecting the multiple particle correlations inside the medium, the effective medium-modified FFs are given as [22,23,25–27]:

$$\tilde{D}_q^h(z_h, Q^2) = D_q^h(z_h, Q^2) + \frac{\alpha_s(Q^2)}{2\pi}\int_0^{Q^2}\frac{\mathrm{d}\ell_T^2}{\ell_T^2} \times \int_{z_h}^1 \frac{\mathrm{d}z}{z}\left[\Delta\gamma_{q\to qg}(z, x, x_L, \ell_T^2) D_q^h(\frac{z_h}{z}, Q^2) + \Delta\gamma_{q\to gq}(z, x, x_L, \ell_T^2) D_g^h(\frac{z_h}{z}, Q^2)\right]. \quad (3)$$

The contribution of the medium-induced gluon radiation is attributed to the medium-modified splitting functions represented by $\Delta\gamma_{q\to qg}$ and $\Delta\gamma_{q\to gq}$. In this formula, we assume that the energy loss of the jet propagating through the medium is totally carried away by the radiative gluons, then the convolution of these energy loss kernels $\Delta\gamma_{q\to qg}$ ($\Delta\gamma_{q\to gq}$) with the (DGLAP) evolved vacuum FFs at any scale $D_{q,g}^h(\frac{z_h}{z}, Q^2)$ implies the assumption that the fast parton first loses its energy in the medium and then fragments into final-state hadrons in vacuum.

The medium-modified splitting functions depend on the properties of the local medium, which cannot be determined directly by the theoretical calculation itself. The jet transport parameter $\hat{q}$, which is defined as the average squared transverse momentum broadening per unit length, is therefore introduced to profile the dependency of the local medium properties in these energy loss kernels [10]. The jet transport parameter $\hat{q}$ can be phenomenologically assumed to be proportional to the local parton density in the hot/dense medium to adopt a further medium description:

$$\hat{q}(\tau, r) = \hat{q}_0 \frac{\rho_{\mathrm{med}}(\tau, r)}{\rho_{\mathrm{med}}(\tau_0, 0)} \cdot \frac{p^\mu u_\mu}{p_0}, \quad (4)$$

where ρ_{med} is the parton (quark and gluon) density in the medium at a given temperature, q_0 is the initial jet transport parameter at the center of the bulk medium at initial time τ_0, p^μ is the four-momentum of the jet and u^μ is the four-flow velocity of the probed local medium in the collision frame. In this article we employ the state-of-art, event-by-event viscous hydrodynamics description IEBE-VISHNU [33] to give the spacetime evolution information of the hot/dense medium, such as temperature, energy density, four-velocity of the local medium at any evolution time and position, and the formation time of QGP, $\tau_0 = 0.6$ fm. Therefore the only undetermined parameter in the calculation is $\hat{q}_0$, representing the strength of the jet–medium interaction, which can be fixed by fitting the data of leading hadrons (usually π meson) suppression in A+A collisions [10,25–27].

When averaging the medium-modified FFs over the initial production position and the jet propagation direction, we are able to directly replace the vacuum FFs in the p+p formalism with these averaged medium-modified FFs $\langle\tilde{D}_c^h(z_h, Q^2, E, b)\rangle$; therefore the formalism of the calculated cross section of the single hadron productions in HIC would take the form of

$$\frac{1}{\langle N_{\mathrm{coll}}^{\mathrm{AB}}(b)\rangle}\frac{\mathrm{d}\sigma_{AB}^h}{\mathrm{d}y\mathrm{d}^2p_T} = \sum_{abcd}\int \mathrm{d}x_a\mathrm{d}x_b f_{a/A}(x_a, \mu^2) f_{b/B}(x_b, \mu^2) \times \frac{\mathrm{d}\sigma}{\mathrm{d}\hat{t}}(ab\to cd)\frac{\langle\tilde{D}_c^h(z_h, Q^2, E, b)\rangle}{\pi z_c} + \mathcal{O}(\alpha_s^3). \quad (5)$$

Here, $\langle N_{\mathrm{coll}}^{\mathrm{AB}}(b)\rangle = \int \mathrm{d}^2r t_A(r) t_B(|\mathbf{b}-\mathbf{r}|)$ is the number of binary nucleon–nucleon collisions at a certain impact parameter b in A+B collisions; it can be calculated by using the Glauber model [44]. $f_{a/A}(x_a, \mu^2)$ represents the effective

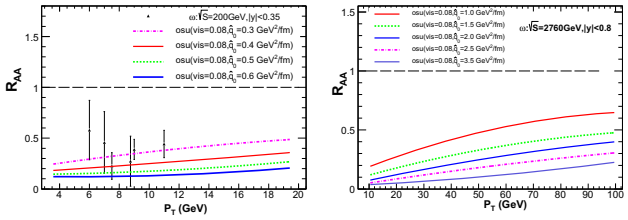

Fig. 5 Left: Comparison between the PHENIX data [15] of the ω nuclear modification factor in Au + Au collisions at 200 GeV and numerical simulations at NLO. Right: The numerical prediction of the ω nuclear modification factor in Pb + Pb collisions at 2760 GeV at NLO

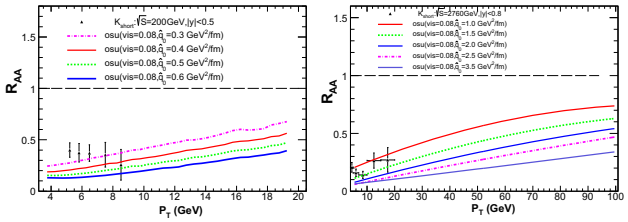

Fig. 6 Left: Comparison between the STAR data [5] of the K^0_S nuclear modification factor in Au + Au collisions at 200 GeV and numerical simulations at NLO. Right: Comparison between the ALICE data [16] of the K^0_S nuclear modification factor in Pb + Pb collisions at 2760 GeV and numerical simulations at NLO

PDFs inside a nucleus. In our calculations, we employed EPPS16 NLO nuclear PDFs [45] to include the initial-state cold nuclear matter effects on single hadron productions [46].

The nuclear modification factor $R_{\rm AA}$ as a function of p_T is calculated as cross sections in A + A collisions divided by the ones in p+p collision, scaled by the averaged number of binary nucleon–nucleon collisions with the chosen impact parameter b [3]:

$$R^b_{AB}(p_T, y) = \frac{d\sigma^h_{AB}/dyd^2p_T}{\langle N^{AB}_{coll}(b)\rangle d\sigma^h_{pp}/dyd^2p_T}\,. \tag{6}$$

The theoretical results of $R_{\rm AA}$ at various values of $\hat{q}_0 = 0.4 - 0.7$ GeV^2/fm for both ω and $K_{\rm s}$ mesons are presented in Figs. 5 and 6.

When obtaining a suitable value of $\hat{q}_0$ by comparing the theoretical calculations of $R_{\rm AA}$ for ω and $K_{\rm s}$ with the corresponding data, there are two caveats. First, since the data of ω and K^0_S meson at large p_T in A+A collisions are rather limited and come with a large uncertainty, it is difficult to make a good constraint on $\hat{q}_0$ with these data. Second, there is the caveat that we employ the IEBE-VISHNU hydrodynamics model to describe the spacetime evolution of the fireball, which gives different information of physics quantities, such as temperature and density, from those provided by other hydro models, such as the Hirano hydro description [31,32]. Therefore, we could not take advantage of the extracted value of $\hat{q}_0$ in Refs. [10,22,23,25–27], where the Hirano hydro description has been utilized.

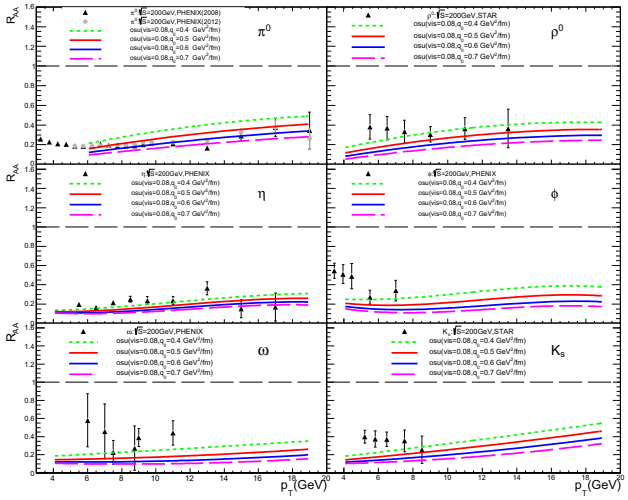

Fig. 7 Theoretical calculation results of nuclear modification factors R_{AA} as functions of $p_{\rm T}$ at $\hat{q}_0 = 0.4 - 0.7$ GeV^2/fm confronted with the RHIC experimental data of π^0 [4,5], ρ^0 [5], K^0_S [5], η [11], ϕ [12], and ω [15]

With these two cautions in mind, and realizing that with our model we are now ready to make a systematic study of six types of identified mesons such as π^0, η, ρ^0, ϕ, ω, and K^0_S in heavy-ion collisions, it will be of great interest to make a global extraction of the jet transport coefficient $\hat{q}_0$ both at RHIC and LHC by confronting our model calculations (with the IEBE-VISHNU hydro model) against all available data on six identified mesons: π^0, η, ρ^0, ϕ, ω, and K^0_S, and then make precise calculations on the nuclear modification factors of these mesons including ω, and K^0_S, and the yield ratios of these six mesons in HIC.

4 Global extraction of $\hat{q}_0$ with $R_{\rm AA}$ for six identified mesons

We perform a systematic calculation of the $R_{\rm AA}$ of 6 identified mesons (π^0, ρ^0, η, ϕ, ω, K^0_S) to compare with all their available experimental data both at RHIC and LHC in Figs. 7 and 8.

In order to extract the best value of the initial jet transport parameter $\hat{q}_0$, we perform a χ^2 fit to compare the theoretical results with different $\hat{q}_0$ and the available experimental data of all the different final hadrons. We have

$$\chi^2(a) = \sum_i \frac{[D_i - T_i(a)]^2}{\sigma_i^2}. \tag{7}$$

In the above equations, D_i represents the experimental grids and T_i is our theoretical prediction at input parameter a. σ_i^2 means the ith systematic and statistical experimental errors. We show in the top panel of Fig. 9 the derived χ^2 averaged by the number of the compared data points for dif-

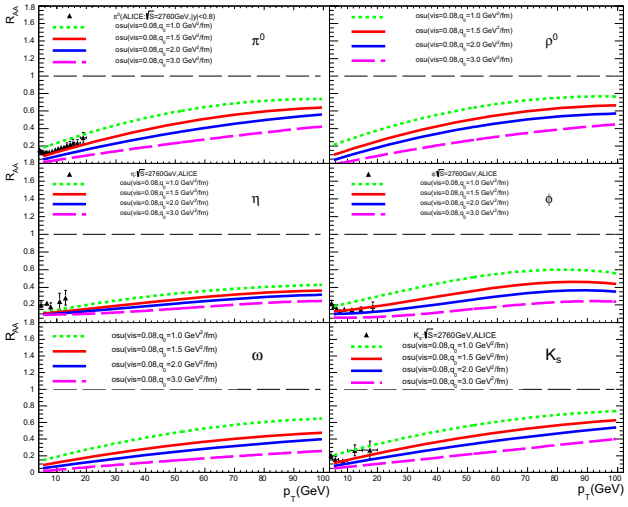

Fig. 8 Theoretical calculation results of nuclear modification factors $R_{\rm AA}$ as functions of $p_{\rm T}$ at $\hat{q}_0 = 1.0 - 3.0$ GeV^2/fm confronted with the LHC experimental data of π^0 [13], η [14], ϕ [16], $K^0_{\rm S}$ [16], ρ^0, and ω

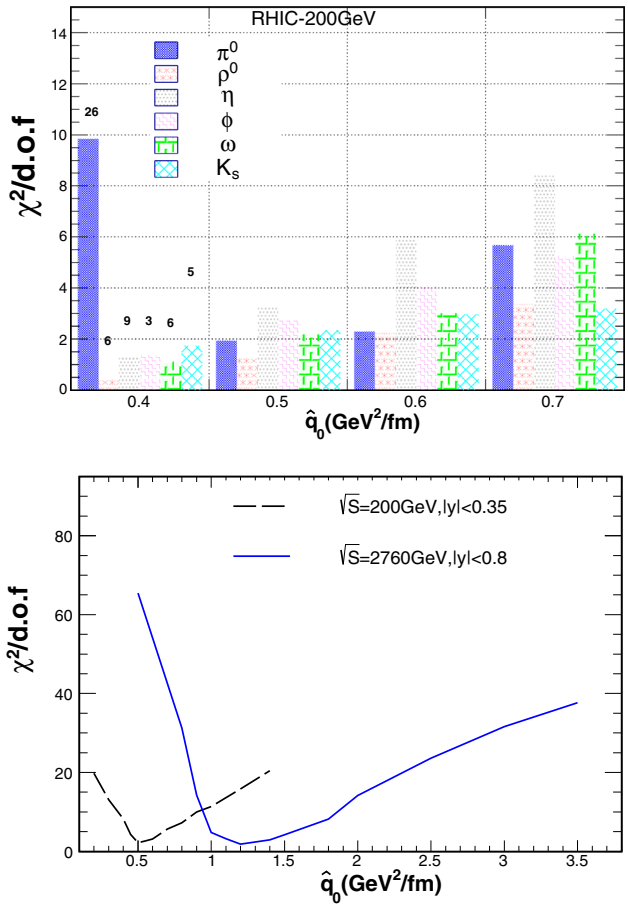

Fig. 9 Top: demonstration of the χ^2/d.o.f between the theoretical prediction for $R_{\rm AA}$ of π^0, ρ^0, η, ϕ, ω, $K^0_{\rm S}$ at different $\hat{q}_0$ and the current public experimental data at the RHIC 200 GeV. Bottom: the global χ^2/d.o.f of R_{AA} taking into account all these six identified hadrons at the RHIC, 200 GeV, and LHC, 2.76 TeV

ferent final-state mesons at various $\hat{q}_0 = 0.4$–0.7 GeV^2/fm at RHIC with $\sqrt{s_{\rm NN}} = 200$ GeV. In the bottom panel of Fig. 9 we plot the curve χ^2/d.o.f as a function of $\hat{q}_0$ both at RHIC and LHC, where the minimum of the curve χ^2/d.o.f with respect to $\hat{q}_0$ presents the best fit of theory with data. We then observe that at RHIC the minimum point of χ^2/d.o.f of all six identified mesons gives the best value of $\hat{q}_0 = 0.5(+0.15/-0.05)$ GeV^2/fm. It is noted that the production of π^0 will carry the largest weight due to its more abundant data with relatively smaller error bars. We also derive the best value of $\hat{q}_0$ in the Pb+Pb collisions at LHC $\sqrt{s_{\rm NN}} = 2.76$ TeV to be $\hat{q}_0 = 1.2(+0.25/-0.15)$ GeV^2/fm, though the curve χ^2/d.o.f at LHC is much flatter that at the RHIC. So theoretical results with $\hat{q}_0 = 1.1 - 1.4$ GeV^2/fm should all give decent descriptions as regards the data at LHC.

It is noted that in our current model the extracted values of jet transport coefficient $\hat{q}_0$ both at RHIC and LHC are smaller than that by the JET Collaboration in Ref. [10] and the ones in our preceding calculations [25–27]. These differences come mainly from the different hydro models utilized in the studies. We have checked [47] that if we employ the Hirano hydro description in the calculation, the extracted values of $\hat{q}_0$ from our global fitting will be consistent with those in Refs. [10,25–27], though the model in this article has the potential to give more precise extraction of the jet transport coefficients when more data of identified hadrons in A+A collisions become available in the near future.

5 Particle ratios of ω/π^0 and K^0_s/π^0 in A+A

With the global extracted value of $\hat{q}_0$ discussed in Sect. 4, we are able to further investigate the particle ratio of ω and $K^0_{\rm S}$ both at RHIC and LHC. We first calculate ω/π^0 ratio as a function of p_T and show the results in p+p and Au+Au at RHIC in the left panel of Fig. 10, where the PHENIX experimental data on the ω/π^0 ratio in p+p are also illustrated. An enhancement of the ratio in A+A relative to that in p+p is found in the small-p_T region, whereas we have a small suppression in the high-p_T regime. We also predict the ω/π^0 ratio as a function of p_T in p+p and Pb+Pb collisions with $\sqrt{s_{NN}} = 2.76$ TeV at LHC. In Fig. 10 we do not see the overlapping of the curves ω/π^0 in p+p and A+A at the high-p_T regime, as we have observed for the ratios η/π^0 [25] and ρ^0/π^0 [26] in p+p and A+A.

To understand this feature deeper, we plot the gluon and quark (fragmentation) contribution fractions to ω (and π^0) in p+p and Au+Au at RHIC in Fig. 11. One sees in the p+p collision at RHIC that the production of ω is dominated by gluon fragmentation. In the A+A collisions, the gluon suffers more energy loss than the light quark due to its larger color factor, which decreases the gluon contribution fraction and increases the light quark contribution fraction, but the

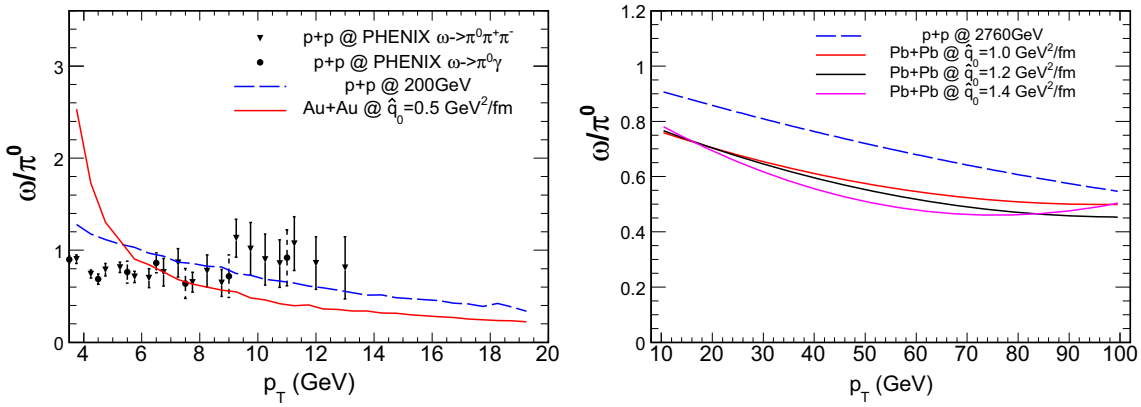

Fig. 10 Left: the yield ratios of ω/π^0 as functions of p_T in p+p and Au+Au collisions with 200 GeV at RHIC, and PHENIX data in p+p [15]. Right: predictions of the yield ratios of ω/π^0 as functions of p_T in p+p and Pb+Pb collisions with 2.76 TeV at LHC

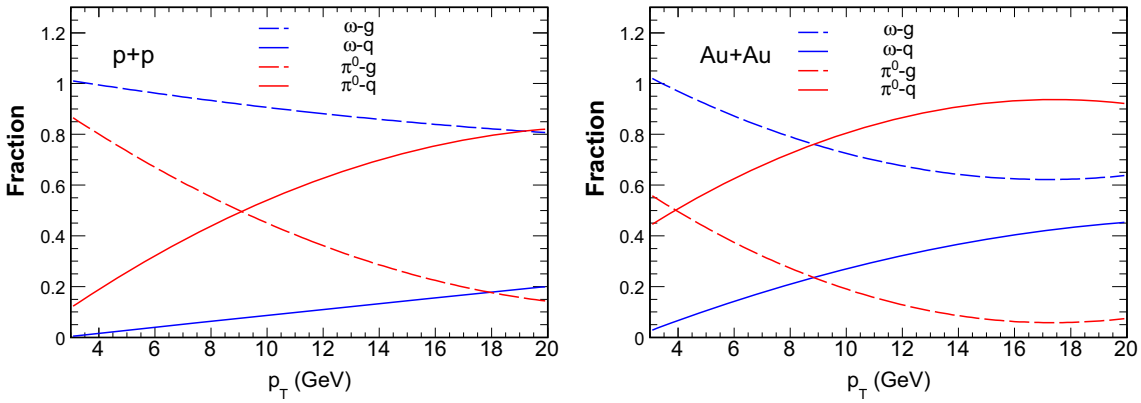

Fig. 11 Gluon and quark contribution fractions of the total yields of ω and π^0 mesons in p+p and Au+Au collisions with $\sqrt{s_{NN}} = 200$ GeV at RHIC

dominant gluon contribution fraction of $\omega \sim 60\%$ is still observed up to $p_T = 20$ GeV in Au+Au at RHIC. On the other hand, π^0 meson production is light quark fragmentation dominant in p+p, and the jet quenching effect further enhances this dominance of light quark fragmentation to π^0 in A+A. Therefore, we see that the yield ratio of ω/π^0 in A+A should be suppressed relative to that in p+p due to the energy loss effect, and it separates from the one in p+p even at very high p_T.

We also compute the K^0_S/π^0 ratio as a function of p_T both at RHIC and LHC in Fig. 12. We find the curves in A+A and in p+p are approaching to each other with p_T increasing, and an obvious coincidence of these two curves is seen at LHC. We show the gluon and quark contribution fractions to the K^0_S meson (and the π^0 meson) as functions of p_T in Fig. 13. We find in p+p collisions that the productions of both K^0_S and π^0 at very large transverse momenta are dominated by quark fragmentation. In A+A collisions, the gluon contribution shall be further suppressed because the gluon generally loses more energy. Thus, both in p+p and A+A collisions, the ratio K^0_S/π^0 should be largely determined by the ratio of quark FFs for K^0_S ($D_q^{K^0_S}(z_h, Q^2)$) to quark FFs for π^0 ($D_q^{\pi^0}(z_h, Q^2)$) at very high p_T, where these FFs vary slowly with the momentum fraction z_h. This is very similar to the case of η_0/π^0 at high p_T [25]. Even though in A+A collisions the jet quenching effect can shift z_h of quark FFs, if the quark FFs have a rather weak dependence on z_h and p_T, we can see that at the very high-p_T regime the curves for K^0_S/π^0 in A+A and p+p come close to each other, and they even coincide at LHC.

6 Summary

In summary, we obtain the NLO FFs of the ω meson in vacuum by evolving the rescaled ω FFs from a broken SU(3) model at a starting scale $Q_0^2 = 1.5$ GeV^2, and we directly employ NLO K^0_S FFs in vacuum from the AKK08 parameterizations; the numerical simulation of productions of both ω and K^0_S matches well with the experimental data in p+p reactions. With the IEBE-VISHNU hydro profile of the QCD

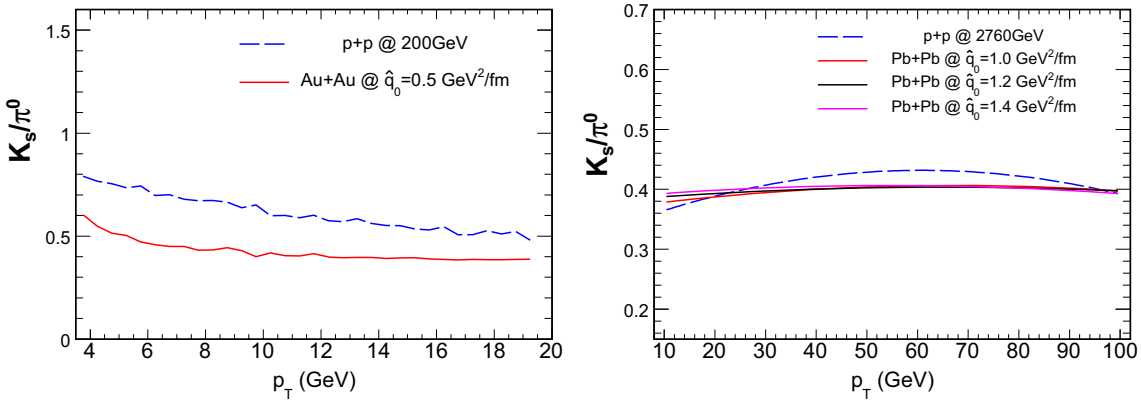

Fig. 12 Left: the production ratios of K_S^0/π^0 as functions of p_T in p+p and Au+Au collisions with 200 GeV at RHIC. Right: predictions of the production ratios of K_S^0/π^0 as functions of p_T in p+p and Pb+Pb collisions with 2.76 TeV at LHC

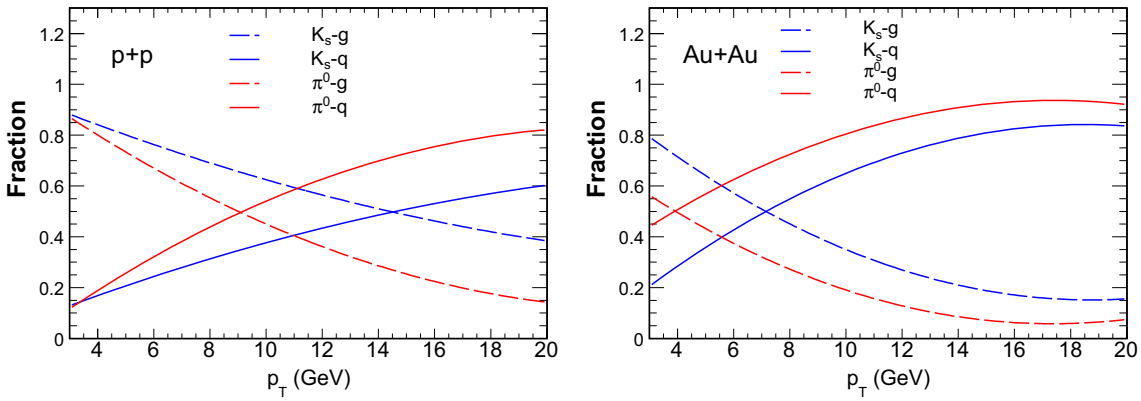

Fig. 13 Gluon and quark contribution fractions of K_S^0 and π^0 yields in $p+p$ and $Au+Au$ collisions with $\sqrt{s_{NN}} = 200$ GeV at RHIC

medium, we calculate the nuclear modification factors of the ω and K_S^0 mesons as well as π^0, η, ϕ, ρ^0 in A+A collisions both at RHIC and LHC, including the jet quenching effect in a higher-twist approach. The global extraction of the jet transport parameter $\hat{q}_0$ is made, with comparison of the theoretical calculation and the experimental data of all six identified mesons: π^0, ρ^0, η, ϕ, ω, K_S^0 . Furthermore, we predict the yield ratios of ω/π^0 both at RHIC and LHC, and a fairly good agreement of the theoretical results and experimental data is found at RHIC. Theoretical predictions of K_S^0/π^0 ratios as functions of p_T at RHIC and LHC are also presented.

Acknowledgements The research is supported by the NSFC of China with Project nos. 11435004 and 11805167, and partly supported by the Fundamental Research Funds for the Central Universities, China University of Geosciences (Wuhan) (no. 162301182691).

Data Availability Statement This manuscript has no associated data or the data will not be deposited. [Authors' comment: This is a theoretical work and no experimental data were used. The reader could contact the corresponding author for numerical results shown in this paper.]

A: Input parameters for ω in broken SU(3) model

See Table 1

Table 1 The parameters for the input fragmentation functions of ω at the initial scale $Q^2 = 1.5\ \mathrm{GeV}^2$ based on broken SU(3) model in our calculation

		ω
V	a	2.16
	b	0.52
	c	1.24
	d	0.27
	e	−0.16
γ	a	2.97
	b	−0.48
	c	5.48
	d	−0.09
	e	1.25
D_g	a	11.67
	b	0.745
	c	3.14
	d	−0.13
	e	−0.21
λ		0.07
θ		40.49
f_g		1.00
f_{sea}		0.99
f_1^u		0.05
f_1^s		0

References

1. X.N. Wang, M. Gyulassy, Phys. Rev. Lett. **68**, 1480 (1992)
2. M. Gyulassy, I. Vitev, X.N. Wang, B.W. Zhang, in Hwa, R.C. (ed.) et al.: Quark Gluon Plasma (pp. 123–191). arXiv:nucl-th/0302077
3. S.S. Adler et al. [PHENIX Collaboration], Phys. Rev. Lett. **96**, 202301 (2006). arXiv:nucl-ex/0601037
4. A. Adare et al. [PHENIX Collaboration], Phys. Rev. Lett. **101**, 232301 (2008). arXiv:0801.4020 [nucl-ex]
5. G. Agakishiev et al. [STAR Collaboration], Phys. Rev. Lett. **108**, 072302 (2012). arXiv:1110.0579 [nucl-ex]
6. A. Adare et al. [PHENIX Collaboration], Phys. Rev. C **88**(2), 024906 (2013). arXiv:1304.3410 [nucl-ex]
7. B.B. Abelev et al. [ALICE Collaboration], Phys. Lett. B **736**, 196 (2014). arXiv:1401.1250 [nucl-ex]
8. S. Acharya et al. [ALICE Collaboration], Eur. Phys. J. C **77**(5), 339 (2017)
9. S. Acharya et al. [ALICE Collaboration], Eur. Phys. J. C **77**(9), 586 (2017). arXiv:1702.00917 [hep-ex]
10. K.M. Burke et al. [JET Collaboration], Phys. Rev. C **90**(1), 014909 (2014). arXiv:1312.5003 [nucl-th]
11. A. Adare et al. [PHENIX Collaboration], Phys. Rev. C **82**, 011902 (2010). arXiv:1005.4916 [nucl-ex]
12. A. Adare et al. [PHENIX Collaboration], Phys. Rev. C **83**, 024909 (2011). arXiv:1004.3532 [nucl-ex]
13. J. Adam et al. [ALICE Collaboration], Phys. Rev. C **93**(3), 034913 (2016). arXiv:1506.07287 [nucl-ex]
14. S. Acharya et al. [ALICE Collaboration], Phys. Rev. C **98**(4), 044901 (2018). arXiv:1803.05490 [nucl-ex]
15. A. Adare et al. [PHENIX Collaboration], Phys. Rev. C **84**, 044902 (2011). arXiv:1105.3467 [nucl-ex]
16. J. Adam et al. [ALICE Collaboration], Phys. Rev. C **95**(6), 064606 (2017). arXiv:1702.00555 [nucl-ex]
17. B.I. Abelev et al. [STAR Collaboration], Phys. Rev. Lett. **97**, 152301 (2006). arXiv:nucl-ex/0606003
18. Y. Xu, J. Phys. G **37**, 094059 (2010). arXiv:1001.3108 [nucl-ex]
19. W. Liu, C.M. Ko, B.W. Zhang, Phys. Rev. C **75**, 051901 (2007)
20. S.J. Brodsky, S. Gardner, Phys. Lett. B **643**, 22 (2006). arXiv:hep-ph/0608219
21. X. Chen, H. Zhang, B.W. Zhang, E. Wang, J. Phys. **37**, 015004 (2010)
22. X. Chen, C. Greiner, E. Wang, X.N. Wang, Z. Xu, Phys. Rev. C **81**, 064908 (2010)
23. X. Chen, T. Hirano, E. Wang, X.N. Wang, H. Zhang, Phys. Rev. C **84**, 034902 (2011)
24. Z.Q. Liu, H. Zhang, B.W. Zhang, E. Wang, Eur. Phys. J. C **76**(1), 20 (2016). arXiv:1506.02840 [nucl-th]
25. W. Dai, X.F. Chen, B.W. Zhang, E. Wang, Phys. Lett. B **750**, 390 (2015). arXiv:1506.00838 [nucl-th]
26. W. Dai, B.W. Zhang, E. Wang, Phys. Rev. C **98**, 024901 (2018)
27. W. Dai, B.W. Zhang, H.Z. Zhang, E. Wang, X.F. Chen, Eur. Phys. J. C **77**(8), 571 (2017). arXiv:1702.01614 [nucl-th]
28. B.W. Zhang, X.N. Wang, Nucl. Phys. A **720**, 429 (2003). arXiv:hep-ph/0301195
29. B.W. Zhang, E. Wang, X.N. Wang, Phys. Rev. Lett. **93**, 072301 (2004). arXiv:nucl-th/0309040
30. A. Schafer, X.N. Wang, B.W. Zhang, Nucl. Phys. A **793**, 128 (2007). arXiv:0704.0106 [hep-ph]
31. T. Hirano, Phys. Rev. C **65**, 011901 (2002). arXiv:nucl-th/0108004
32. T. Hirano, K. Tsuda, Phys. Rev. C **66**, 054905 (2002). arXiv:nucl-th/0205043
33. C. Shen, Z. Qiu, H. Song, J. Bernhard, S. Bass, U. Heinz, Comput. Phys. Commun. **199**, 61 (2016)
34. D. Peresunko [ALICE Collaboration], Nucl. Phys. A **904-905**, 755c (2013). arXiv:1210.5749 [nucl-ex]
35. B.I. Abelev et al. [STAR Collaboration], Phys. Rev. C **75**, 064901 (2007). arXiv:nucl-ex/0607033
36. N. Kidonakis, J.F. Owens, Phys. Rev. D **63**, 054019 (2001). arXiv:hep-ph/0007268
37. T.J. Hou et al., JHEP **1703**, 099 (2017). arXiv:1607.06066 [hep-ph]
38. S. Albino, B.A. Kniehl, G. Kramer, Nucl. Phys. B **803**, 42 (2008). arXiv:0803.2768 [hep-ph]
39. D. Indumathi, H. Saveetha, Int. J. Mod. Phys. A **27**, 1250103 (2012). arXiv:1102.5594 [hep-ph]
40. H. Saveetha, D. Indumathi, S. Mitra, Int. J. Mod. Phys. A **29**(07), 1450049 (2014). arXiv:1309.2134 [hep-ph]
41. M. Hirai, S. Kumano, Comput. Phys. Commun. **183**, 1002 (2012). arXiv:1106.1553 [hep-ph]
42. X.F. Guo, X.N. Wang, Phys. Rev. Lett. **85**, 3591 (2000). arXiv:hep-ph/0005044
43. X.N. Wang, X.F. Guo, Nucl. Phys. A **696**, 788 (2001). arXiv:hep-ph/0102230
44. D.G. d'Enterria, arXiv:nucl-ex/0302016
45. K.J. Eskola, P. Paakkinen, H. Paukkunen, C.A. Salgado, Eur. Phys. J. C **77**(3), 163 (2017). arXiv:1612.05741 [hep-ph]
46. S.Y. Chen, K.M. Shen, W. Dai, B.W. Zhang, H.Z. Zhang, E.K. Wang, Commun. Theor. Phys. **64**(1), 95 (2015)
47. B.W. Zhang, G.Y. Ma, W. Dai, S. Wang, S.L. Zhang, arXiv:1811.12093 [nucl-th]